Self-Assembled Monolayers of Parent and Derivatized [n]Staffane-3,3$^{(n-1)}$-dithiols on Polycrystalline Gold Electrodes

Yaw S. Obeng,[†] Mark E. Laing,[‡] Andrienne C. Friedli, Huey C. Yang, Dongni Wang,[§] Erik W. Thulstrup,[‖] Allen J. Bard,* and Josef Michl*,[⊥]

Contribution from the Department of Chemistry and Biochemistry, The University of Texas at Austin, Austin, Texas 78712-1167. Received April 2, 1992

Abstract: Synthesis of the terminally disubstituted rigid rod molecules, [n]staffane-3,3$^{(n-1)}$-dithiols, $n = 1-4$, and their singly functionalized derivatives carrying an acetyl or a pentaammineruthenium(II), [Ru(NH$_3$)$_5$]$^{2+}$, substituent is described. Self-assembled monolayers of the neat [n]staffane derivatives and of their mixtures with *n*-alkyl thiols were prepared on polycrystalline gold electrodes. Grazing incidence FTIR spectroscopy and comparison with polarized IR spectra of model compounds oriented in stretched polyethylene revealed that, in the films assembled directly from the dithiols, the average orientation of the [n]staffane rods was halfway between perpendicular and parallel to the surface, whereas, in the films obtained from the singly functionalized derivatives, the rods were nearly perpendicular to the surface. The degree of ordering and packing was also investigated by contact angle measurements with deionized water. The electrode blocking properties of the films were investigated by three independent electrochemical techniques, cyclic voltammetry in a solution containing K$_4$Fe(CN)$_6$, chronoamperometry in a solution of Ru(NH$_3$)$_6$Cl$_3$, and cyclic voltammetry of the gold surface in sulfuric acid. The results from the three methods were in good agreement and showed that the films assembled from the dithiols were not as well organized as those obtained from the monoderivatized analogues. In situ hydrolytic removal of the protective acetyl groups and subsequent functionalization of the resultant film covered with free thiol groups with aquapentaammineruthenium(II), [Ru(NH$_3$)$_5$(H$_2$O)]$^{2+}$, are possible without disturbing the structure of the film. Electrodes covered with monolayers carrying ruthenium pentaammine groups on their outer surface exhibit oxidation–reduction waves at 0.51 V vs SCE attributable to the Ru(II)–Ru(III) couple, demonstrating electron transfer across the monolayer. The formal potential of the immobilized couple is about 60-mV more positive than that of the dissolved complex, [[(NH$_3$)$_5$Ru]–[n]staffanedithiol]$^{2+}$, in 1 M HClO$_4$ solution. The surface concentration of Ru is the same in the films assembled from this complex and those produced by in situ functionalization of a film covered with free thiol groups and corresponds to a monolayer of (NH$_3$)$_5$Ru. However, in the former type of film, the surface concentration of the staffane rods is only about half of that in the latter, implying that only about half of the surface thiol groups have been metalated.

Introduction

Terminally disubstituted [n]staffanes ([n]1) were originally developed for use as assembly elements in a molecular-size "Tinkertoy" construction set[1–4] but can also be viewed simply as a new class of straight and fairly rigid inert spacers suitable for investigations of electron and energy transfer. In this regard, terminal disubstitution with thiol-based groups[3–5] is particularly interesting, and preliminary results of an optical investigation of intramolecular electron transfer between Ru(II) and Ru(III) attached to 3,3$^{(n-1)}$-bis(methylthio)[n]staffanes ([n]3, $n = 1,2$), generated in situ from the isovalent species [n]2, have been presented elsewhere.[6] In this paper, we describe the formation of self-assembled monolayers of neat [n]staffane-3,3$^{(n-1)}$-dithiols ([n]4), thiol–thiol acetates (monothiols, [n]5), and thiol–ruthenium pentaammine thiols ([n]6) (Figure 1) on gold electrodes ($n = 1-4$), as well as mixed films formed with *n*-alkanethiols. We find that careful basic hydrolysis converts films of [n]5 undamaged

*To whom correspondence should be addressed.
[†] Present address: AT&T Bell Labs, Allentown, PA 18103.
[‡] Present address: Unilever Research, Port Sunlight Laboratory, Quarry Road East, Bebington, Wirral L63 3JW, England.
[§] Present address: Chemistry Department, The Royal Veterinary and Agricultural University, DK-1871 Frederiksberg, Denmark.
[‖] Present address: Institute I, Roskilde University, DK-4000 Roskilde, Denmark.
[⊥] Present address: Department of Chemistry and Biochemistry, University of Colorado, Boulder, CO 80309-0215.

(1) (a) Kaszynski, P.; Michl, J. *J. Am. Chem. Soc.* **1988**, *110*, 5225. (b) Kaszynski, P.; Friedli, A. C.; Michl, J. *Mol. Cryst. Liq. Cryst. Lett. Sect.* **1988**, *6*, 27.
(2) Michl, J.; Kaszynski, P.; Friedli, A. C.; Murthy, G. S.; Yang, H.-C.; Robinson, R. E.; McMurdie, N. D.; Kim, T. In *Strain and Its Implications in Organic Chemistry*; de Meijere, A., Blechert, S., Eds.; NATO ASI Series; Kluwer Academic Publishers: Dordrecht, The Netherlands, 1989; Vol. 273, p 463.
(3) Friedli, A. C.; Kaszynski, P.; Michl, J. *Tetrahedron Lett.* **1989**, *30*, 455.
(4) Kaszynski, P.; Friedli, A. C.; Mich, J. *J. Am. Chem. Soc.* **1992**, *114*, 601.
(5) (a) Bunz, V.; Polborn, K.; Wagner, H.-V.; Szeimes, G. *Chem. Ber.* **1988**, *121*, 1785. (b) Wiberg, H. B.; Waddell, S. T. *J. Am. Chem. Soc.* **1990**, *112*, 2194.
(6) (a) Michl, J.; Friedli, A. C.; Obeng, Y. S.; Bard, A. J. *Proceedings of the Sixth International Conference on Energy and Electron Transfer*; Fiala, J.; Pokorny, J., Eds.; Charles University: Prague, Czechoslovakia, 1989. The rates reported in this paper are too high due to the use of an erroneous literature equation for data treatment. The correct rate constants are 1 × 10^7 and 2 × 10^6 s^{-1} for [1]3 and [2]3, respectively, in 0.1 M DCl in D$_2$O. (b) Positions on the individual bicyclo[1.1.1]pentane cages in an [n]staffane are distinguished by the number of primes, from no primes at one of the terminal cages to $n - 1$ primes on the other terminal cage. Thus, the terminal bridgehead positions in [2]staffane are 3 and 3′, in [3]staffane, 3 and 3″, and in [n]staffane, 3 and 3 with $n - 1$ primes, indicated by 3$^{(n-1)}$, following the usage common in mathematics.
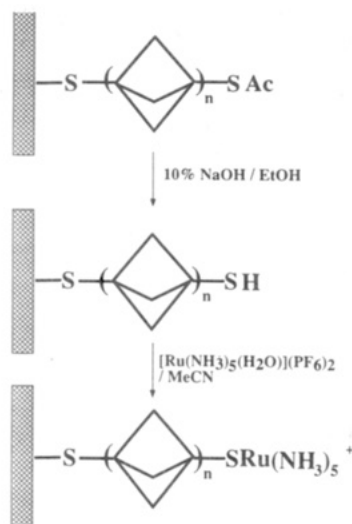
Figure 1. Schematic representation of the chemical transformations of a film of type A into a film of type E.

into films of [**n**]**4** and characterize the structures and the electrochemical properties of all of these.   The formation of a self-

	X	Y	film type
[n]1	H	H	
[n]2	[(NH$_3$)$_5$RuMeS]$^{2+}$	[(NH$_3$)$_5$RuMeS]$^{2+}$	
[n]3	[(NH$_3$)$_5$RuMeS]$^{2+}$	[(NH$_3$)$_5$RuMeS]$^{3+}$	
[n]4	HS	HS	A, C
[n]5	HS	CH$_3$COS	B
[n]6	HS	[(NH$_3$)$_5$RuS]$^{2+}$	D, E, F
[n]7	CH$_3$COS	CH$_3$COS	

assembled monolayer relies upon direct adsorption onto substrates from solution and differs from the well-known Langmuir–Blodgett technique of monolayer preparation where highly ordered monolayers or systems of monolayers on solid supports are produced by mechanical transfer of preformed films from a liquid–air interface. Monolamellar self-assembled films have been used as interfaces for a wide variety of studies, e.g., in corrosion inhibition,[7] tribology,[8] and catalysis.[9] Polycrystalline gold substrates were used as electrodes because the well-known strong specific interaction of gold with sulfur facilitates self-assembly.[10–14]

Experimental Section

Materials. 18 MΩ-cm Milli-Q water (Milli Q, El Paso, TX) was used throughout this study for washings, solution preparation, and contact angle measurements.   The electrolytes used were all reagent grade.

(7) Bregman, J. I. *Corrosion Inhibitors*; MacMillan: New York, 1963; Chapter 5, p 197.

(8) (a) Bowden, F. B.; Tabor, D. *The Friction and Lubrication of Solids*; Oxford University Press: London, 1968; Part II, Chapter 19. (b) Zisman, N. A. In *Friction and Wear*; Davies, R., Ed.; Elsevier: New York, 1959.

(9) (a) Murray, R. W. In *Electroanalytical Chemistry*; Bard, A. J., Ed.; Marcel Dekker: New York, 1984; Vol. 13. (b) Durrand, R. R.; Bencosme, C. S.; Collman, J. P.; Anson, F. C. *J. Am. Chem. Soc.* **1983**, *105*, 2710.

(10) Tillman, N.; Ulman, A.; Elman, J. F. *Langmuir* **1989**, *5*, 1020.

(11) Nuzzo, R. G.; Allara, J. L. *J. Am. Chem. Soc.* **1983**, *105*, 4481.

(12) (a) Bain, C. D.; Troughton, E. B.; Tao, Y.-T.; Evall, J.; Whitesides, G. M.; Nuzzo, R. G. *J. Am. Chem. Soc.* **1989**, *111*, 321. (b) Whitesides, G. M.; Laibinis, P. E. *Langmuir* **1990**, *6*, 87. (c) Strong, L.; Whitesides, G. M. *Langmuir* **1988**, *4*, 546. (d) Ogletree, D. F.; Ocal, C.; Marchon, B.; Somorjai, G. A.; Salmeron, M.; Beebe, T.; Siekhaus, W. *J. Vac. Sci. Technol., A.* **1990**, *8*, 297.

(13) Facci, J. S.; Falcigno, P. A.; Gold, J. M. *Langmuir* **1986**, *2*, 732. Porter, M. D.; Bright, T. B.; Allara, D. L.; Chidsey, C. E. D. *J. Am. Chem. Soc.* **1987**, *109*, 3559.

(14) (a) Finklea, H. O.; Avery, S. Lynch, M. *Langmuir* **1987**, *3*, 409. (b) Moaz, R.; Sagiv, J. *J. Colloid Interface Sci.* **1984**, *100*, 456. (c) Finklea, H. O.; Hanshew, D. D. *J. Am. Chem. Soc.* **1992**, *114*, 3173.

Absolute ethanol (Aaper Alcohol and Chemical Co., Shelbyville, KY), acetonitrile (Fisher Scientific), and acetone (Mallinkrodt, Paris, KY) were used as received.

Equipment and Measurements. Melting points were determined using a Boetius PHMK05 apparatus, with microscope attachment, at a warm-up rate of 4 °C min^{-1} or in a sealed capillary and are uncorrected. Boiling points are also uncorrected. NMR spectra were run at 360 MHz in CDCl$_3$ on a Nicolet NT-360 instrument, unless specified otherwise. Chemical ionization (CI) and electron impact (EI) mass spectra were obtained on Bell & Howell 21-491 and VG ZAB-2E spectrometers, respectively. Elemental analyses were performed at Atlantic Microlabs, Norcross, GA. Preparative gas chromatography was performed on 6-ft SE-30 20% on Chromosorb column.

Infrared (IR) spectra of 3,3$^{(n-1)}$-bis(acetylthio)[n]staffanes[3,4] ([**n**]**7**, $n = 1$–4), aligned in stretched polyethylene, were recorded at room temperature in the 400–2000-cm^{-1} region on a Perkin-Elmer 1702 FTIR instrument equipped with a SPECAC Model KRS-5 linear polarizer in the sample beam. The resulting spectra, $E_Z(\tilde{\nu})$, with the electric vector parallel to the polymer-stretching direction, and $E_Y(\tilde{\nu})$, with the electric vector perpendicular to this direction, were base-line corrected. Narrow regions near 730 and 1480 cm^{-1} were blocked by the absorption of the polymer.

The polymer sheets were prepared by cutting a 2-mm thick wall of a polyethylene laboratory bottle (Kartell, Germany), heating it to 150 °C and quenching it in cold water to improve its optical quality, and then stretching it to 400% of its original length. The stretched sheet was kept in a concentrated solution of the staffane derivative in chloroform at 40 °C for up to 24 h, until a desired optical density of the solute was achieved. This had no significant effect on the degree of alignment of the polymer.

All other infrared spectra were recorded at 4-cm^{-1} resolution on a Nicolet 60SXR FTIR instrument using a HgCdTe detector cooled with liquid nitrogen. Isotropic spectra were measured in KBr pellets unless stated otherwise. Grazing incidence measurements on films deposited on a 1 × 1-in. Au-coated glass were performed at an incidence angle of 84°, using a Harrick model RMA-00G reflection attachment and a wire grid polarizer (IGP225, Cambridge Physical Science). Typically 4000 scans were recorded.

Cyclic voltammetry measurements were performed with a PAR system (model 175 universal programmer and 173 potentiostat) and a Houston Instruments 200 X-Y recorder. In chronoamperometric experiments, current transients were stored on a Norland 3001 digital oscilloscope or were obtained with a BAS 100-B electrochemical analyzer interfaced to an IBM–XT personal computer. Transient data were recorded at several different sampling rates for each modified electrode to obtain an accurate digitized current over the entire time window.[15] Either a saturated calomel electrode (SCE) or a silver wire quasi-reference electrode (QRE) was used as the reference electrode, and platinum gauze served as the auxiliary electrode in all of the electrochemical experiments. All electrochemical measurements were made at room temperature (24 ± 2 °C).

Contact angle measurements were made with a Ramé-Hart Model 100 goniometer equipped with a tilting stage. A sessile 10-μL drop of Milli Q water was dropped from a microsyringe onto the sample and the contact angle measured. The stage was then inclined to 45°, and the receding and advancing contact angles were measured. The reported values are the average of at least three different measurements in every case.

General Synthetic Procedure for Monothiols ([n]5). 3,3$^{(n-1)}$-Bis(acetylthio)[n]staffane ([**n**]**7**)[3,4] (in most cases 1 mmol) was dissolved in degassed ethanol (10 mL/1 mmol) under argon. One equivalent of KOH in ethanol was added dropwise. For $n = 3$ and $n = 4$ oligomers, the reaction was carried out in gently refluxing ethanol and in 2-propanol, respectively, to improve solubility. The solvent was then evaporated, and equal volumes of water and methylene chloride were added. Acidification with acetic acid under argon gave milky layers, which were separated, and the aqueous layer was extracted three times with methylene chloride. The combined organic layers were dried with Na$_2$SO$_4$ and evaporated to give dithiol, monothiol, and starting material in statistical proportions (1:2:1, respectively, except for the case of $n = 1$, where monothiol predominated) by GC analysis. After evaporation of solvent, the products were separated and purified by column chromatography on silica gel (3% ethyl acetate in hexanes eluent) and then sublimation. Preparative GC could also be used when $n < 3$, but significant decomposition resulted with higher oligomers.

(15) (a) Gueshi, T.; Tokuda, K.; Matsuda, H. *J. Electroanal. Chem.* **1978**, *89*, 247. (b) Tokuda, K.; Gueshi, T.; Matsuda, H. *J. Electroanal. Chem.* **1979**, *101*, 29. (c) Tokuda, K.; Gueshi, T.; Matsuda, H. *J. Electroanal. Chem.* **1979**, *102*, 41. (d) Leddy, J.; Bard, A. J. *J. Electroanal. Chem.* **1983**, *153*, 223.

[n]Staffane-3,3(r−1)-Dithiols

J. Am. Chem. Soc., Vol. 114, No. 25, 1992 9945

General Synthetic Procedure for Dithiols ([n]4). When only the dithiol was required, the above procedure was followed using 2 equiv or excess of base. Purification was simplified greatly to Kugelrohr distillation (n = 1), flash column chromatography on silica gel with 10% ethyl acetate in hexanes eluent, or sublimation (n > 1). Yields are reported for dithiols prepared with this method.

Bicyclo[1.1.1]pentane-1,3-dithiol ([1]4).[5a] Volatile liquid with a strong stench; yield 78%; bp 170–180 °C (Kugelrohr); ^{1}H NMR δ 2.11 (s, 2 H), 2.18 (s, 6 H); ^{13}C NMR δ 34.97, 62.19; IR (CHCl₃) 2974, 2914, 2877, 1209, 1049, 943, 789 cm⁻¹; EIMS m/z (intensity) 131 (M − 1, 3) 99 (M − SH, 32), 82 (40), 74 (100), 73 (70), 45 (48).

3-(Acetylthio)bicyclo[1.1.1]pentane-1-thiol ([1]5). Yield 72%; bp 50–60 °C (50 Torr, sublimator); ^{1}H NMR δ 2.17 (s, 1 H), 2.26 (s, 3 H), 2.35 (s, 6 H); ^{13}C NMR δ 31.02, 37.50, 38.01, 59.95, 195.75; IR (CCl₄) 2995, 2930, 1702 (C=O), 1205, 1120, 941 cm⁻¹; EIMS m/z 131 (M − Ac, 8), 99 (M − SAc, 9), 58 (17), 45 (13), 43 (100); CIMS 175 (M + 1, 59), 141 (78), 131 (14), 99 (100); CI HRMS m/z (Calcd for C₇H₁₁OS₂, 175.0251) 175.0236. Anal. Calcd for C₇H₁₀OS₂: C, 48.24; H, 5.78; S, 36.79. Found: C, 48.27; H, 5.76; S, 36.75.

[2]Staffane-3,3′-dithiol ([2]4).[5a] Yield 72%; mp 126–127 °C (lit[5a] 98–105 °C); subl 70 °C (0.5 Torr); ^{1}H NMR δ 1.82 (s, 12 H), 1.99 (s, 2 H); ^{13}C NMR δ 34.80, 39.98, 55.69; IR 2979, 2906, 2671, 1209, 1147, 892 cm⁻¹; EIMS m/z 165 (M − SH, 1), 131 (22), 125 (31), 91 (100), 65 (21), 59 (51), 45 (59); CIMS m/z 199 (M + 1, 16), 167 (24), 163 (18), 132 (24), 131 (100), 125 (26), 105 (17). Anal. Calcd for C₁₀H₁₄S₂: C, 60.56; H, 7.11; S, 32.33. Found: C, 60.48; H, 7.11; S, 32.23.

3′-(Acetylthio)[2]staffane-3-thiol ([2]5). Yield 40%; mp 74–75 °C; subl (65 °C, 0.25 Torr); ^{1}H NMR δ 1.85 (s, 6 H), 2.00 (s, 6 H), 2.02 (s, 1 H), 2.26 (s, 3 H); ^{13}C NMR δ 31.24, 34.86, 37.99, 40.09, 42.80, 53.54, 55.74, 196.35; IR 2974, 2908, 2871, 1688 (C=O), 1211, 1119, 957, 894 cm⁻¹; EIMS m/z 207 (M − SH, 1), 197, (M − Ac, 4), 165 (16), 163 (14), 149 (20), 131 (26), 91 (40), 59 (23), 43 (100); CIMS m/z 241 (M + 1, 8), 165 (52), 131 (100), 77 (45), 65 (75); HRMS m/z (Calcd for C₁₂H₁₆OS₂, 240.0643) 240.0646. Anal. Calcd for C₁₂H₁₆OS₂: C, 59.96; H, 6.71; S, 26.67. Found: C, 60.06; H, 6.72; S, 26.59.

[3]Staffane-3,3″-dithiol ([3]4). Yield 69%; mp 194–195 °C; subl 100 °C (0.7 Torr); ^{1}H NMR δ 1.42 (s, 6 H), 1.79 (s, 12 H), 1.97 (s, 2 H); ^{13}C NMR δ 34.70, 37.56, 40.79, 48.38, 55.51; IR 2964, 2904, 2871, 1209, 1190, 1052, 892 cm⁻¹; EIMS m/z 264 (M, 2), 231 (M − SH, 6), 141 (57), 129 (69), 91 (100); CIMS m/z 265 (M + 1, 68), 263 (M − 1, 68), 231 (M − SH, 100), 229 (74); HRMS m/z (calcd for C₁₅H₂₀S₂ 264.1006) 264.1008. Anal. Calcd for C₁₅H₂₀S₂: C, 68.13; H, 7.62; S, 24.25. Found: C, 68.14; H, 7.66; S, 24.17.

3″-(Acetylthio)[3]staffane-3-thiol ([3]5). Yield 38%; mp 125–126 °C; subl 105 °C (0.7 Torr); ^{1}H NMR δ 1.45 (s, 6 H), 1.79 (s, 6 H), 1.96 (s, 6 H), 1.98 (s, 1 H), 2.25 (s, 3 H); ^{13}C NMR δ 31.14, 34.75, 37.65, 37.71, 38.01, 40.79, 43.65, 48.52, 53.51, 55.64, 196.20; IR 2964, 2905, 2872, 1692 (C=O), 1208, 1114, 889, 628 cm⁻¹; EIMS m/z 306 (M, 3), 263 (M − Ac, 4), 231 (M − SAc, 15), 125 (45), 91 (38), 59 (19), 43 (100); HRMS m/z (calcd for C₁₇H₂₂OS₂, 306.1112) 306.1125. Anal. Calcd for C₁₇H₂₂OS₂: C, 66.63; H, 7.23; S, 20.92. Found: C, 66.51; H, 7.28; S, 20.83.

[4]Staffane-3,3‴-dithiol ([4]4). Used without sublimation; yield 80%; mp 192–193 °C; ^{1}H NMR δ 1.38 (s, 12 H), 1.79 (s, 12 H), 1.97 (s, 2 H); ^{13}C NMR δ 34.66, 37.28, 38.19, 40.91, 48.03, 55.50; IR 2964; 2906, 2871, 1211, 1085; 895 cm⁻¹; EIMS m/z 330 (M, 9), 297 (M − SH, 4), 129 (39), 125 (73), 115 (36), 105 (40), 91 (100), 79 (38), 77 (39), 59 (41); HRMS m/z (calcd for C₂₀H₂₆S₂, 330.1476) 330.1465.

3‴-(Acetylthio)[4]staffane-3-thiol ([4]5). Used without sublimation; yield 23%; mp > 200 °C (decomposition without melting); ^{1}H NMR δ 1.39 (s, 6 H), 1.41 (s, 6 H), 1.78 (s, 6 H), 1.96 (s, 6 H), 1.97 (s, 1 H), 2.24 (s, 3 H); ^{13}C NMR δ 31.26, 34.64, 37.27, 37.39, 37.89, 38.20 (2 C's), 40.91, 43.80, 48.04 (6 C's, two internal cages) 53.31, 55.49, 196.68; IR 2964, 2906, 2871, 1694 (C=O), 1213, 1120, 1051, 630 cm⁻¹; EIMS m/z 372 (M, 8), 357 (M − Me, 7), 297 (M − SAc, 14), 157 (32), 143 (31), 129 (46), 128 (38), 125 (93), 105 (34), 91 (49), 43 (100); HRMS m/z (calcd for C₂₂H₂₈OS₂, 372.1582) 372.1579.

The purity of the products was checked by GLC.

Ru Complexes. Mononuclear ruthenium complexes, [n]6, were prepared from the staffanedithiol [n]3 and separated as hexafluorophosphate (PF₆⁻) salts by following published procedures.[16] The presence of the −SRu(NH₃)₅²⁺ ion was verified by cyclic voltammetry at a glassy carbon electrode without further characterization.

Substrate Preparation. For IR and electrochemical studies, 99.999% gold was sputtered on glass (borosilicate glass, 2.5 × 7.5 cm²), in a MRC (Materials Research Corporation, Orangeburg, NY) Model 8620 sputtering system at 10⁻² Torr, with an RF power of 150 W and an RF peak-to-peak voltage of 1.8 kV, using an aluminum mask. The glass

substrate was cleaned prior to deposition in a fresh mixture of 1:3 v/v H₂O₂ (30%)/H₂SO₄ (96%) for 30 min, rinsed with water followed by ethanol, dried in an oven at 160 °C, and then subjected to 2 min of argon plasma etching prior to sputtering.[17] The glass was primed with a ~50-Å Cr layer followed by a ~2000-Å Au layer. This afforded Au disk electrodes with a mean geometric area of 0.18 cm². Electrical contact was made to the working electrode via an alligator clip at a larger rectangular gold patch which was ~2 cm from the disk. The electrodes were examined by STM and appeared to have irregularly shaped domains that are relatively flat at the nanometer level, separated by nanometer-size valleys.

The gold substrates were either used immediately or were carefully wrapped in lint-free lens paper for storage in a desiccator. The stored substrates were used within 48 h and were cleaned by ~1-min immersion in hot chromic acid or 1:3 H₂O₂/H₂SO₄ followed by copious rinsing with water and absolute ethanol and then dried under a jet of dry, filtered argon gas just before use.[17] Freshly deposited or cleaned substrates were hydrophilic (H₂O contact angle < 25°), but they slowly turned hydrophobic in air (the contact angle after 24 h was ~70°). Both cleaning methods afforded identical surface characteristics for the bare substrate as well as the subsequent modified electrodes.

Film Preparation. Metal-free staffane self-assembled films were made by immersing freshly deposited or freshly cleaned gold substrates in ~1 mM solutions of [n]4 (film type A) or [n]5 (film type B) in EtOH for ~24 h, rinsed copiously with fresh portions of EtOH, and Ar dried. Films of the ruthenium-derivatized staffanes were prepared by three different routes:

(i) **Self-Assembly of Neat Films of [n]6.** Mononuclear Ru–staffane complexes, [n]6, were dissolved in MeCN to afford ~1 mM solutions, and the clean gold substrates was introduced to yield a film of type D. Self assembly was allowed (~24 h) to reach equilibrium, and the electrodes were washed with MeCN, water, and EtOH.

(ii) **In-Situ Synthesis of [n]6.** Clean polycrystalline gold substrates were immersed in 20 μM solutions of [n]5 in absolute EtOH for ~18 h, rinsed copiously with fresh portions of absolute ethanol, and then Ar dried. The resultant electrode was relatively hydrophobic. The dry electrode was exposed to 2–5% NaOH in EtOH for ~1 min and rinsed thoroughly with water and absolute EtOH.[18] As shown by FTIR measurements, this treatment hydrolyzes the thiol acetate functional group to afford a thiol surface that is hydrophilic (film type C). The substrate was then exposed to ~5 mM aquapentaammineruthenium(II) hexafluorophosphate, [Ru(NH₃)₅(H₂O)](PF₆)₂, in degassed MeCN overnight, washed with fresh portions of MeCN, water, and EtOH, and then Ar dried to yield film type E. The sequence of transformations is summarized in Figure 1.

(iii) **Coassembly of [n]6 and an Alkanethiol (RSH).** Clean polycrystalline gold substrates were exposed to a [n]6/RSH (R = C₅H₁₁, C₈H₁₇, or C₁₀H₂₁) solution (1:10 molar ratio) overnight (total concentration ~5 mM), to yield film type F. The assembled films were then exposed to a neat 0.1 mM solution of RSH in MeCN for 8 h. This step was carried out to exchange [n]6 molecules adsorbed at defect sites, grain boundaries, or film layers adsorbed onto the primary monolayer for RSH and was intended to produce films that do not contain electroactive groups in metastable environments.[19-23]

Results and Discussion

In the following, we first describe the preparation of monolayer films (A–F) and then the results of the structural characterization of the monolayers A–E by IR spectroscopy and the monolayers A–F by contact angle measurements and then present the results of the electrode blocking experiments. We conclude with the results of the electrochemical experiments on the pentaammine-ruthenium(II)-tagged films D and E. The monolayer films were generally very stable. For example, they could undergo over 100

(16) Stein, C. A.; Taube, H. *J. Am. Chem. Soc.* **1981**, *103*, 693.

(17) Goss, C. A.; Charych, D. H.; Majda, M. *Anal. Chem.* **1991**, *63*, 85.
(18) Greene, T. W.; Werts, P. G. M. *Protective Groups in Organic Synthesis*; J. Wiley & Sons: New York, 1991.
(19) Creager, S. E.; Rowe, G. K. *Anal. Chim. Acta* **1991**, *246*, 233.
(20) Creager, S. E.; Collard, D. M.; Fox, M. A. *Langmuir* **1990**, *6*, 1617.
(21) Collard, D. M.; Fox, M. A. *Langmuir* **1991**, *7*, 1192.
(22) Sabatini, E.; Moaz, R.; Sagiv, J.; Rubinstein, I. *J. Electroanal. Chem.* **1989**, *219*, 365.
(23) (a) Kwang, W. S. V.; Atannasoska, L. Miller, L. *Langmuir* **1991**, *7*, 1419. (b) Chidsey, C. E. D.; Loiacono, D. N.; Sleator, T.; Nakahara, S. *Surf. Sci.* **1988**, *200*, 45. (c) Chidsey, C. E. D.; Loiacono, D. N. *Langmuir* **1990**, *6*, 682. (d) Chidsey, C. E. D.; Bertozzi, C. R.; Puvinski, T. M.; Mujsce, A. M. *J. Am. Chem. Soc.* **1990**, *112*, 4301. (e) Chidsey, C. E. D. *Science* **1991**, 919.

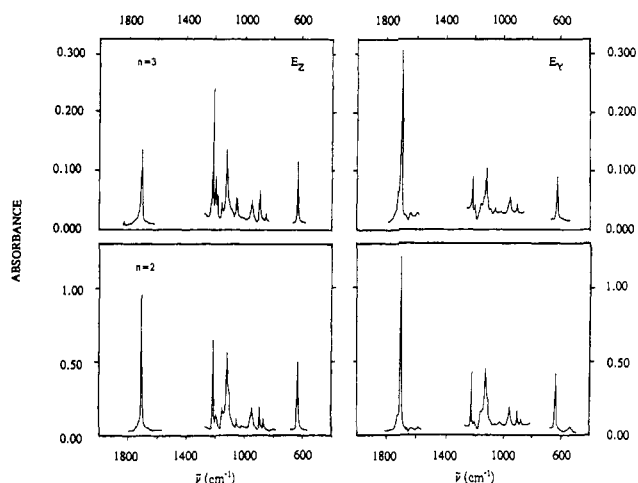**Figure 2.** IR linear dichroism of 3,3$^{(r-1)}$-bis(acetylthio)[n]staffanes, n = 2 and 3, in stretched polyethylene: E_Z (E_Y), absorbance polarized parallel (perpendicular) to the stretching direction.

Table I. IR Linear Dichroism of 3,3$^{(r-1)}$-Bis(acetylthio)[n]staffanes [n]7

n = 1		n = 2		n = 3		n = 4	
$\bar{\nu}^a$	K^b	$\bar{\nu}^a$	K^b	$\bar{\nu}^a$	K^b	$\bar{\nu}^a$	K^b
627	0.39	628	0.38	629	0.42	629	0.47
		869	0.48	847			
931	0.43	895	0.46	892	0.63	892	~0.7
946	0.36	946	0.36	946	0.37	948	0.33
1030	0.28	1051		1050	~0.66		
1117	0.38	1115	0.39	1117	0.42	1117	0.49
1140	0.34	1145	0.37	1147			
		1188	0.49	1190	0.63	1198	~0.6
1204	0.40	1211	0.44	1210	0.64	1213	0.64
1704	0.31	1704	0.28	1702	0.18	1699	0.18

^{a}cm^{-1}. ^{b}Orientation factor (see text).

scans in cyclic voltammetry (100 mV s^{-1}) without change or could be transferred from one supporting electrolyte solution to another without loss.

Preparation of Monolayer Films. Dithiols [n]4 and singly acetylated thiols [n]5 were synthesized from the readily available 3,3$^{(r-1)}$-bis(acetylthio)[n]staffanes [n]7$^{1-4}$ by basic hydrolysis. This procedure appears preferable to alternative methods reported[5] for the preparation of bridgehead bicyclo[1.1.1]pentanethiols. Purification was most easily achieved by elution through a silica gel column. The resulting mono- and dithiols were moderately sensitive to air oxidation and were generally dissolved in degassed ethanol solutions immediately after preparation and stored in a freezer. All compounds decompose slowly in the solid state; even in the freezer under argon some yellowing occurred. As evidence of physical changes, the melting points become lower, with melting occurring over a broader range with gradual decomposition. Elemental analyses remain accurate, however.

We have prepared three kinds of metal-free (A, B, C) and three kinds of ruthenium-containing (D, E, F) monolayers, obtained as follows: A, self-assembly from the dithiols, [n]4 (n = 2–4); B, self-assembly from the thiol–thiol acetates, [n]5 (n = 2–4, Figure 1); C, hydrolytic removal of surface acetate groups from the monolayer B (n = 2–4, Figure 1); D, self-assembly from the thiol–thiol (pentaammine)ruthenium(II) complexes, [n]6 (n = 2–4); E, reaction of the monolayer C with aquapentaammine-ruthenium(II) (n = 2–4, Figure 1); F, self-assembly from mixtures of the complexes [n]6 and alkanethiol, (n = 2–4).

Attempts to derivatize the dithiol monolayers A with aquapentaammineruthenium(II) did not yield reproducible results.

IR Spectra. **(i) Transition Moment Directions from Measurements on [n]7.** To interpret the IR spectra of the films in terms of molecular orientation, a few characteristic and intense vibrations of the [n]staffane skeleton need to be identified and their polarization determined. Given the 3-fold symmetry of a rigid [n]staffane hydrocarbon,[24] the allowed IR vibrations will be polarized either along the long axis or in the plane perpendicular to it, and the latter will be degenerate. The terminal substituents present in our molecules will lower the overall symmetry, but the transition moment directions of the vibrations of the skeleton itself will be dictated by the high local symmetry, so that the "parallel"–"perpendicular" nomenclature will apply.

Incorporation in stretched polyethylene represents a well-established means of aligning nonpolar molecules for dichroic spectroscopy.[25] We have chosen the diacetylated dithiols [n]7,

n = 1–4, as typical, stable in air, and suitable for incorporation in stretched polyethylene. Figure 2 shows the IR absorption spectra of two of the molecules, polarized parallel (E_Z) and perpendicular (E_Y) to the polymer stretching direction. The C–H stretching region was blocked by the absorption of the polymer itself.

The dichroic ratio $d_i = E_Z(i)E_Y(i)$ was converted into the orientation factor $K_i = d_i/(2 + d_i)$ for each observed transition i in the usual fashion[25] (Table I). The physical significance of these values is $K_i = \langle \cos^2 \alpha_i \rangle$, where α_i is the angle between the ith transition moment and the stretching direction of the polymer and the pointed brackets indicate averaging over all observed molecules. Thus, large K_i values are characteristic of transitions polarized close to the effective orientation axis of the solute molecule, and small ones indicate transitions polarized at a large angle to it. The effective orientation axis is that direction in the molecular framework that has the largest $\langle \cos^2 \alpha \rangle$ value.

The spectra of all four molecules are very similar, but the orientation factors vary significantly along the series (Table I, Figure 2) and demonstrate an increasing degree of average alignment of the effective orientation axis of the solute with the stretching direction of the polymer. This was expected, as all prior experience with the method[25] shows that the location of the effective orientation axis in the molecule, as well as its degree of alignment, is primarily determined by molecular shape. As the molecules become gradually more rodlike[26] upon going from [1]7 to [4]7, the orientation axis is expected to approach the 3-fold symmetry axis of the [n]staffane skeleton and to line up better with the polymer-stretching direction.

Comparison with the IR spectra of [n]staffane hydrocarbons[24] and consideration of vibrations associated with the thiol acetate group identify the intense peak near 1210 cm^{-1} as characteristic of the [n]staffane skeleton. The orientation factors listed in Table I leave no doubt that this vibration is long-axis polarized. In the following, we shall use the intensity of this parallel vibration and those of the C–H stretching vibrations at 2850–3000 cm^{-1}, which must clearly be of perpendicular polarization in view of the orientation of the CH$_2$ groups within the [n]staffane skeleton, to determine the orientation of [n]staffane rods in thin films.

(ii) Grazing Incidence IR Spectra of Monolayer Films. The results for both staffane lengths, n = 2 and 3, are identical, and it seems safe to assume that the same results would be obtained for the longer staffanes. IR absorption spectra of the immobilized monolayers on a reflecting metal surface are distorted relative to solution spectra in ways that are fairly well understood,[27] and such distortions are also manifested in our spectra. In particular, the monolayer absorption peaks, primarily the broader ones, are shifted to somewhat higher frequencies, and in our spectra, this is most clearly apparent for the carbonyl stretch. Also, in some cases, reflection is actually weakly enhanced, so that the absorption peaks appear with a negative amplitude. In our spectra, this is barely detectable in the CH stretching region and not seen

(24) (a) Murthy, G. S.; Hassenrück, K.; Lynch, V. M.; Michl, J. *J. Am. Chem. Soc.* **1989**, *111*, 7262. (b) Gudipati, M. S.; Hamrock, S. J.; Balaji, V.; Michl, J. *J. Phys. Chem.*, in press.

(25) Michl, J.; Thulstrup, E. W. *Spectroscopy with Polarized Light. Solute Alignment by Photoselection in Liquid Crystals, Polymers, and Membranes*; VCH Publishers: Deerfield Beach, Florida, 1986.

(26) Friedli, A. C.; Lynch, V. M.; Kaszynski, P.; Michl, J. *Acta Crystallogr., B* **1990**, *46*, 377.

(27) Allara, D.; Baca, A.; Pryde, C. A. *Macromolecules* **1978**, *11*, 1215.
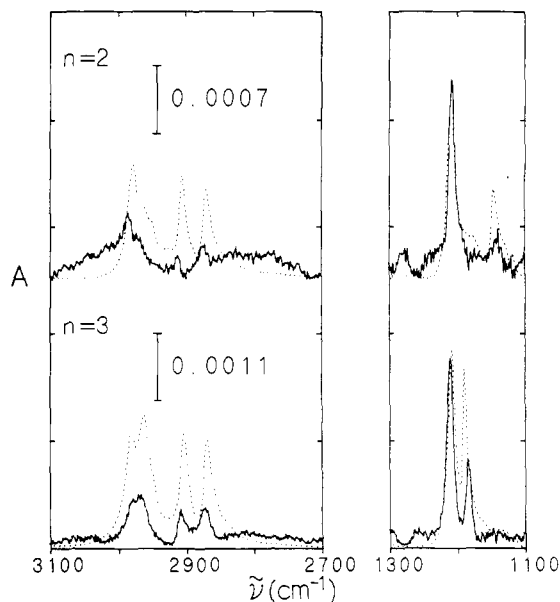
Figure 3. Grazing incidence IR absorption spectra of monolayers of type A on a gold substrate: dotted line, isotropic spectrum in a KBr pellet, plotted on a scale such as to make the intensity of the 1210-cm^{-1} peak equal to that in the film.
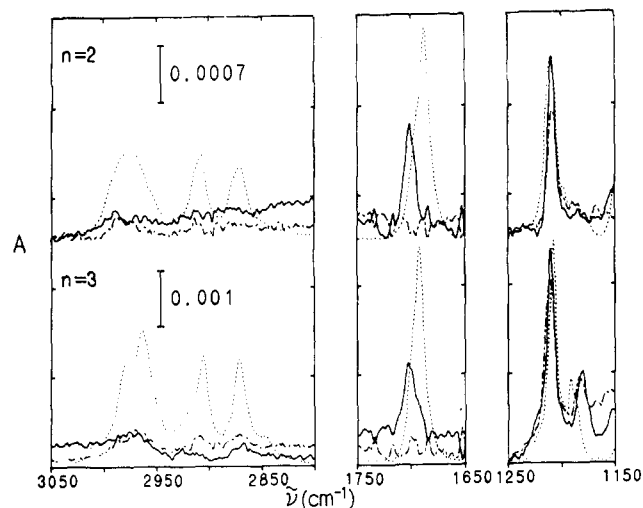

Figure 4. Grazing incidence IR absorption spectra of monolayers of types B (solid line) and C (dash-dotted line) on a gold substrate: dotted line, isotropic spectrum of the thiol acetate [n]5 in a KBr pellet, plotted on a scale such as to make the intensity of the 1210-cm^{-1} peak equal to that in the film of type B.

elsewhere. These anomalies, and the relatively low signal-to-noise ratio, call for caution in any quantitative interpretation of the results, and we suspect that the orientation of molecular axes cannot be determined with an accuracy better than ±10°.

In a molecule located next to a conductor surface, only that component of a transition dipole that is perpendicular to the surface contributes to light absorption to the first approximation, due to the effect of image charges in the conductor. If the organization of the molecules near the surface is not isotropic, those transitions whose polarization directions in the molecular frame tend to lie parallel to the surface will have relatively reduced intensity. In our case, these are the staffane CH$_2$ stretching vibrations, and we conclude that, on the average, the long axes of the molecules in monolayer A form a small angle with the normal; i.e., the molecules are "standing up" on the surface. We cannot distinguish from these measurements between a situation in which some of them are standing up absolutely straight while others are lying down and a situation in which all of them are standing up but not quite straight. To obtain quantitative information on molecular orientation in the films from the relative intensities of the 2850–3000 and 1210-cm^{-1} vibrations, the gold surface is assumed to be perfectly flat.

(iii) Monolayers of Type A. Figure 3 shows selected regions of the grazing incidence of the IR absorption spectra of monolayers of type A on a gold substrate for n = 2 and 3. The ordinary isotropic IR absorption spectra recorded in KBr pellets are shown as well. The integrated intensities of the CH stretches relative to those of the 1210-cm^{-1} band are smaller in the monolayer spectra by a factor of about 0.37 in the case of n = 2 and a factor of about 0.49 in the case of n = 3. Allowing for the degeneracy of the short-axis polarized transitions, we obtain an average of 45° and 40° for n = 3 and 2, respectively, for the angle between the [n]staffane long axis and the surface normal. It is clear that, in the films of type A, the average inclination of the [n]staffane rods is about halfway between normal and parallel to the surface.

(iv) Monolayers of Types B and C. Figure 4 shows the spectra of films of types B and C. In the spectra of the former, the central region contains a C=O stretching vibration near 1700 cm^{-1}. The polarization direction of the carbonyl stretch can be expected to lie close to the C=O bond direction, but its orientation relative to the molecular axis will be a function of the molecular conformation. The C–H stretching intensity due to the methyl group is difficult to separate reliably from that due to the [n]staffane CH$_2$ groups but is likely to be relatively small, particularly for n = 3.

Within our experimental accuracy, the CH stretching bands either are absent altogether or are present as weak negative peaks in the spectra of the monolayers self-assembled from the thiol–thiol acetates [n]5, whether before hydrolysis (type B) or after hydrolysis (type C). The observed spectra represent an extreme case of the situation encountered with monolayers of type A, and in the first approximation, the molecules in the films of types B and C are standing with their long axes normal to the surface. There is no detectable difference between the alignment of the [n]staffane cores in the films of types B and C, suggesting that the hydrolytic step does not perturb the structure of the monolayer. The somewhat reduced absorption intensity of the 1210-cm^{-1} band in the spectrum of films C relative to films B is reproducible, and we suspect that it is due to the perturbations of the IR transition moment by the electric fields due to the acetyl substituent charge distribution and its mirror image in the metal. There is no reason to think that it is due to partial destruction of the monolayer and removal of some of the staffane rods upon going from film B to C. As we shall see below, film C conserves excellent blocking properties, and upon going to film E, the intensity of the 1210-cm^{-1} band increases again, even above that of film B.

The integrated intensity of the carbonyl stretch band in film B relative to that of the 1210-cm^{-1} peak is smaller by a factor of about 0.62 for n = 2 and 0.41 for n = 3 when compared with the spectra of the isotropic samples. This result contains information on the average conformation of the acetylthio group in the monolayer. A priori, one would expect it to be either cis planar, with the CSCO dihedral angle ϕ equal to zero (the O atom pointing to the metal surface and the CH$_3$ group outward), or trans planar, ϕ = 180°, (the O atom pointing outward and the CH$_3$ group toward the metal).

Relative to that of the 1210-cm^{-1} peak, which is polarized along the molecular long axis and thus normal to the surface, the intensity of the carbonyl stretching vibration is reduced in the film spectrum by a factor of $\langle \cos^2 \sigma \rangle$. The pointed brackets indicate ensemble averaging and σ is the angle between the surface normal and the C=O bond.

Some of the variation in the intensity ratio observed between n = 2 and 3 may be due to the effects just discussed for the 1210-cm^{-1} band, and some may reflect real conformational differences. In view of the uncertainties in the interpretation of intensity differences, we prefer not to attempt an analysis of minor effects. We assume that the C=O bonds in all the thioacetyl groups in the film make the same angle σ with the surface normal and take $|\cos \sigma|$ to be equal to 0.7 ± 0.1.

Two ranges of CSCO dihedral angles are compatible with the observations. They are particularly simple to derive if the staffane

rods are assumed to be exactly perpendicular to the surface and if the bridgehead C–S bond is oriented exactly along the long axis of the molecule. Then, the angle ω between the S–CO bond and the surface normal is equal to the CSC valence angle. If the SCO valence angle is labeled ρ, trigonometry yields

$$\cos \phi = (\cos \omega \cos \rho - \cos \sigma)/\sin \omega \sin \rho$$

The use of the average values of the valence angles obtained from single-crystal X-ray structures of the bis(acetylthio) derivatives [2]7, [3]7, and [4]7,[26] $\omega = 102.5°$ and $\rho = 123.0°$, yields two solutions: (i) $\phi = 0$–29° and (ii) $\phi = 126$–146°.

In the single-crystal structures, the bridgehead C–S bond is bent backward, away from the acetyl group, and in some cases, the staffane rod itself is slightly bent in the same direction as well. This distortion is presumably due to the need to accommodate the neighboring molecules. If a similar need exists in the packed monolayer at all, it is likely to be less severe. If the resulting tilt of the bridgehead C–S bond from the surface normal away from the acetyl group is τ, the proper value to use for ω in the calculation of the dihedral angle ϕ becomes the sum of the CSC valence angle and the tilt angle τ. The tilt reduces the magnitude of permitted values of ϕ somewhat. For instance, for a tilt of $\tau = 5°$, the permitted ranges of ϕ are (i) 0–17° and (ii) 123–143°.

Two ranges of the dihedral angle ϕ characterizing the acetylthio group are compatible with observations: (i) cis, with ϕ possibly deviating from zero by perhaps as much as 30° (carbonyl oxygen pointing inward), and (ii) approximately gauche, with ϕ about 120–150°. The planar or nearly planar conformation (i) is normal for the acetylthio group, is similar to the single-crystal structures of the bis(acetylthio) derivatives,[26] and is quite plausible. The twisted conformation (ii), although compatible with the IR intensity ratios, appears highly improbable. The trans conformation (carbonyl oxygen pointing outward) is excluded.

The striking difference in the average orientation of the [n]-staffane rods in the films of types A and B is most readily rationalized by postulating that the favored mode of attachment of the thiol sulfur to the gold surface is with the C–S bond normal to the surface, presumably pointing into the center of a triangle formed by three gold atoms, and that this mode of attachment, characteristic of films B and C, is also used by about half of the staffanedithiol molecules in the films of type A. An attachment with the C–S bond parallel to the surface requires a sulfur-to-surface distance of about 2.7–3.0 Å, imposed by the thickness of the [n]staffane rod,[26] and is apparently only about half as favorable, since in films A the formation of two such bonds, one on each rod end, seems to compete about evenly with the favored mode of attachment. Although we have no experimental evidence for such bimodal orientation distribution in films A in the absence of Raman spectra, it appears more reasonable than other possibilities compatible with the observed average angle. It is difficult to see why a different angle of inclination would be favored by the gold-attached thiol group depending on the presence or absence of an acetyl protecting group on the distant terminus of the rod, if that other terminus did not interact with the gold surface.

(v) Monolayers of Types D and E. Figure 5 shows the grazing incidence IR spectra of monolayers of types D and E. As would be expected, these are dominated by bands due to the five ammonia molecules present on each ruthenium atom: the broad N–H stretching band between 3000 and 3400 cm^{-1}, the degenerate deformation band near 1600 cm^{-1}, and the symmetric deformation band at 1333 cm^{-1}.[28] The Ru–S stretching vibration lies outside our observation range, and we have no information on the C–S–Ru angle. The three C–H stretching bands of the [n]staffane rods are again absent within our detection ability, demonstrating that, in films D and E, the rods are still standing perpendicular to the surface.

There is one striking and reproducible difference between the two spectra shown in Figure 5, however. While the ammonia peaks have a comparable intensity in both, suggesting equal surface
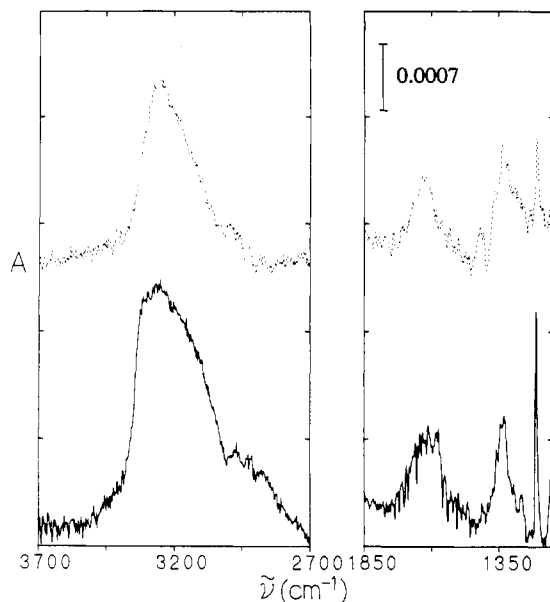

Figure 5. Grazing incidence IR absorption spectra of monolayers of types D (dotted line) and E (solid line) on a gold substrate.

coverage by ruthenium pentaammine, the long-axis polarized 1210-cm^{-1} peak characteristic of the [n]staffane rod is weaker in the film of type D by a factor of at least 2. Since the rods are oriented equally in both films, the large intensity difference is best attributed to a difference in their numbers.

This actually is to be expected and is consistent with the electrochemical surface coverage measurement discussed below. The radius of the staffane rod in the monolayer is probably close to 2.9 Å, judging by the crystal structures of a series of substituted staffanes[26] and by the 26 Å^2 per molecule area in the Langmuir–Blodgett monolayer of staffane-3-carboxylates,[29] and that of the roughly spherical ruthenium pentaammine unit is closer to 3.5 Å.[30] Since the C–S bond is perpendicular to the surface, the packing of the staffanes is probably commensurate with that of the gold lattice with the S located at a 3-fold site. In the absence of $Ru(NH_3)_5^{2+}$ substitution, we would expect a closer packing that accommodates the molecular area. However, in the ruthenation step in which type E films are produced, the densest commensurate packing is $2(\sqrt{3} \times \sqrt{3})$ and at least half of the staffane rods must remain metal-free. The actual packing by $Ru(NH_3)_5^{2+}$ may well be less dense because of electrostatic repulsions among these positively charged centers.

By the same token, self-assembly from [n]6 cannot pack the ruthenium pentaammine termini any closer than $2(\sqrt{3} \times \sqrt{3})$, and the packing density of the staffane rods underneath is at best half that found in films of type E. It is not certain how the voids in film D are filled, but a likely possibility is the counterions. There is no evidence for water in the IR spectra of dried films.

As we shall see below, electrochemical measurements provide independent evidence that the coverage with Ru atoms is the same in films D and E, supporting the conclusion drawn here from the approximate equality of the ammonia IR bands in the two spectra. The existence of such independent evidence is reassuring in view of the disquieting variation of the 1210 cm^{-1} band intensity between films B and C. Comparison of Figures 4 and 5 shows that the conversion of film C into E is associated with an increase in the 1210 cm^{-1} band intensity, even above that of film B. However, we find it unlikely that the reproducible difference in the intensity of this peak in films D and E could be wholly due to the same effect. Still, we are sufficiently concerned about these intensity variations that we hesitate to interpret the ratio of the two as representing quantitatively the ratio of the staffane rod densities

(28) Nakamoto, K. *Infrared and Raman Spectra of Inorganic and Co-ordination Compounds*; Wiley: New York, 1986.

(29) Yang, H. C.; Magnera, T. F.; Lee, C.; Bard, A. J.; Michl, J. *Langmuir*, in press.

(30) Meyer, T. J. *Acc. Chem. Res.* **1978**, *11*, 94.

Table II. Contact Angle of Water on the Monolayer Modified Electrodes[a]

type[b]	n[c]	θ[d]	θ_a	θ_r
A	1	62 ± 2	66 ± 2	52 ± 2
	2	85 ± 2	69 ± 2	87 ± 2
	3	76 ± 2	69 ± 2	80 ± 2
	4	81 ± 2	69 ± 2	86 ± 2
B	2	78 ± 2	67 ± 2	80 ± 2
	3	74 ± 2	61 ± 2	84 ± 2
	4	74 ± 2	66 ± 2	84 ± 2
C	1	26 ± 2	20 ± 2	27 ± 2
	2	38 ± 10	34 ± 2	38 ± 10
	3	43 ± 9	39 ± 2	43 ± 5
D	2	63 ± 2	61 ± 2	66 ± 2
	3	63 ± 2	51 ± 2	65 ± 2
E	2	42 ± 6	36 ± 6	44 ± 6
	3	53 ± 4	51 ± 1	60 ± 1
F	1/C$_5$H$_{11}$SH	38 ± 11	29 ± 11	44 ± 11
	2/C$_5$H$_{11}$SH	67 ± 7	62 ± 5	69 ± 8
	3/C$_8$H$_{17}$SH	78 ± 11	67 ± 9	82 ± 12

[a] A sessile 10-μL drop of Milli-Q water. [b] Film types: A = [n]4, dithiol; B = [n]5, thiol–thiol acetate; C = [n]4, dithiol, D,E = [n]6, ruthenium complex; F = [n]6 and RSH, mixed film. [c] Number of repeat units in rod. [d] The stationary contact angles (θ, deg) were measured with stage normal, while the advancing (θ_a, deg) and receding (θ_r, deg) contact angles were measured with the sample inclined at 45°.

on the surface in the films D and E.

(vi) Contact Angle Measurements. The results of contact angle measurements obtained with deionized water (pH = 5.5) on the various films support the structural assignments based on IR (Table II). The values for the thiol–thiol acetates [n]5, type B, are high, as would be expected for a surface covered with methyl groups. They are in relatively good agreement with the angle (70°) reported for the aliphatic thiol–thiol acetate HS(CH$_2$)$_{12}$SCOC-H$_3$.[12b] The dithiol films of type A show even higher contact angles than the films of type B, in keeping with the notion that about half of the staffane rods lie flat on the surface, exposing much pure hydrocarbon surface to the contacting solution. The thiol-terminated films of type C (derived from the thiol acetate) have low contact angles, again not surprisingly.

The contact angles obtained on Ru-containing films of types D and E were essentially the same within experimental error but depended on the length of the staffane rods. The small differences between films D and E are not understood. Both films were more hydrophilic than films A and B, and in contrast to the purely organic films, both the pure and mixed films containing staffanes derivatized with ruthenium showed higher uncertainty in the observed contact angle, indicating rather heterogeneous surfaces.[12b] The surface heterogeneity can be explained in terms of irregularities in the distribution of the counterions and the Ru(NH$_3$)$_5$$^{2+}$ moieties over the film. The apparent dependence of the contact angles on the staffane rod length suggests that the contact angle is sensitive to the underlying substrate.[31]

(vii) Blocking Properties of the Films. The cyclic voltammetric current–potential (*i-E*) responses for a bare gold electrode (solid line) in a 1.2 mM solution of Fe(CN)$_6$$^{4-}$ with 0.1 M KCl are shown in Figure 6. The corresponding cyclic voltammograms for an electrode with a blocking monolayer of a film of type A ([4]4) and an electrode with a blocking monolayer of film type B ([4]5) are also shown. A strong decrease in both the oxidation and reduction waves is apparent for the type B monolayer. The monolayer of type A does not block the solution redox reaction nearly as efficiently; the oxidation and reduction waves decreased by ~70%. The same finding was made for all A, B pairs (at all chain lengths). Voltammograms obtained with films of type C were identical to those of type B.

In an attempt to obtain a quantitative measure of the area of the electrode that remained exposed after the monolayer film had been prepared, current transients were recorded both at the bare and blocked electrodes in a 10 mM solution of Ru(NH$_3$)$_6$Cl$_3$ in
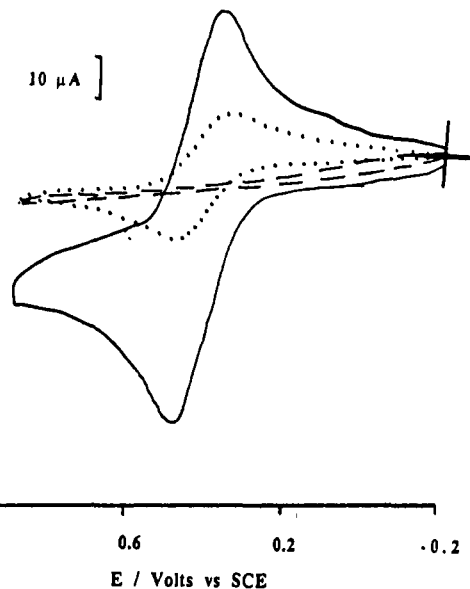
(31) Walczak, M. M.; Chung, C.; Stole, S. M.; Widrig, C. A.; Porter, M. C. *J. Am. Chem. Soc.* **1991**, *113*, 2370.

Figure 6. Cyclic voltammogram of a 1.2 mM solution of K$_4$Fe(CN)$_6$·3H$_2$O at a bare gold electrode (solid line), a gold electrode with a monolayer of [4]5 (type B, dashed line), and a gold electrode with a monolayer of [4]4 (type A, dotted line). Scan rate 50 mV s^{-1}, SCE reference electrode.
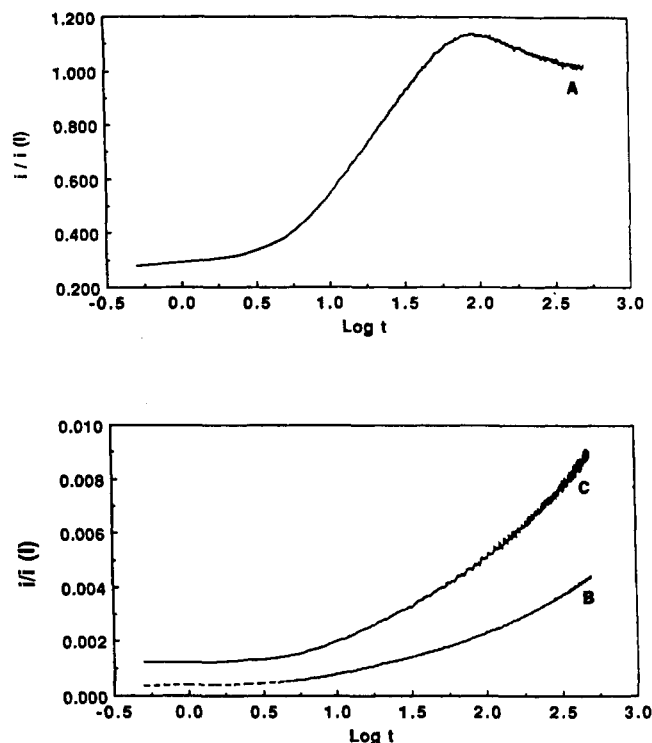

Figure 7. Plot of the current transient at an electrode with a monolayer of [3]4 (film type A) and of [3]5 (films of type B and C, respectively), normalized to the current transient at a bare gold electrode vs log (time) in a 10 mM solution of Ru(NH$_3$)$_6$Cl$_3$ (0.1 M H$_2$SO$_4$).

0.5 M H$_2$SO$_4$ for films of types A, B, and C, each for n = 1–4, as well as with film types D and E (n = 2, 3). These were then analyzed according to the pinhole model proposed by Matsuda et al.[15] In this model, the chronoamperometric behavior of the diffusing reactants is described at a partially coated electrode; the amount of the electrode left exposed is obtained from the short time limit of a plot of the current at a modified electrode divided by the semi-infinite diffusion current obtained at a bare electrode.[15c,d] Figure 7 shows such a plot for electrodes with blocking monolayers of types A, B, and C. The short time results suggest that the exposed area is about 30% of the total electrode area for film A but less than 1% for the films B and C. The blocking

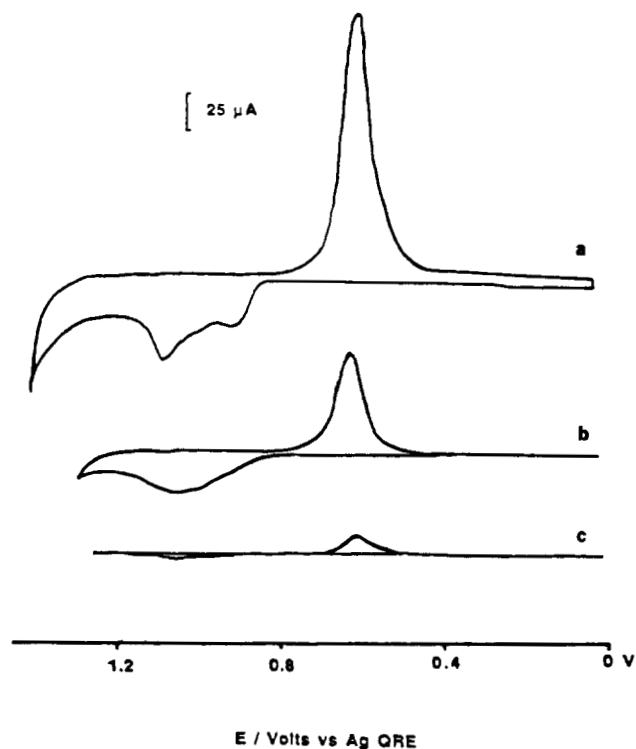9950   *J. Am. Chem. Soc., Vol. 114, No. 25, 1992*

Obeng et al.

Figure 8. Gold surface oxidation and reduction waves (a) at a bare gold electrode, (b) with a monolayer of [3]4 (film type A), and (c) with a monolayer of [3]5 (film type E) in ~0.1 M H_2SO_4, pH 1.6, $\nu = 50$ mV s^{-1}.

Figure 9. Cyclic voltammogram of (a) [2]6 (film type E) on a polycrystalline gold substrate (geometric area = 0.18 cm^2) and (b) a 2 mM solution of [2]6 with a glassy carbon electrode, in 1 M $HClO_4$, $\nu = 200$ mV s^{-1}, with a SCE reference electrode.

efficacy of the monolayer films decreases with decreasing staffane length for $n \leq 2$. For the films B and C, the blocking is ~95% for $n = 2$ and ~99% for the longer staffanes. For $n = 1$, blocking films were not obtained. The apparent blocking efficiency by the Ru-containing films was lower: ~70% for type E ($n = 2,3$) and ~55% for type D ($n = 2$). The low efficiency found with the type E film compared to the much better efficiency for the precursor type C film suggests that the coordinated $Ru(NH_3)_5^{2+}$ groups in the type E film may be partially mediating electron transfer to the solution probe species and the actual coverage and direct blocking may be higher.

An alternative method for the determination of blocking efficiency, based upon the decrease in the gold oxide reduction wave, has also been used as a direct measure of the degree of blocking in self-assembled monolayers.[22] Figure 8a shows the oxidation and reduction waves obtained at a bare gold electrode in H_2SO_4 at pH = 1.6, Figure 8b shows the corresponding cyclic voltammogram for a gold electrode covered with a self-assembled film of type A, and Figure 8c shows the cyclic voltammogram obtained with a monolayer of type B or C, which gave identical results. If the potential was scanned positive of +1.7 V vs a Ag QRE, the monolayer was destroyed, presumably due to oxidation of the gold-bound sulfur, and the film no longer blocked the electrode.

The results for each of the compounds calculated using the three methods are in relatively good agreement. In general, the films of type A were found to only block 60–80% of the gold oxide reduction peak and solution redox reaction, compared to the >95% blocking of the gold oxide reduction and solution redox reaction by films of types B and C. The less effective blocking of the electrode surface by the films of type A is consistent with the FTIR structural evidence discussed above. If about half of the molecules are present with both thiol groups chemisorbed on the gold surface, in a more or less random fashion, and about half are standing upright, the rods are likely to be disorganized, with the probability of a greater number of pinholes relative to that for the films of type B and C.

That the film type A may not be coherent is further indicated by the fact that redox waves for the $Ru^{2+/3+}$ couple were not reproducibly obtained when the type A films were derivatized with

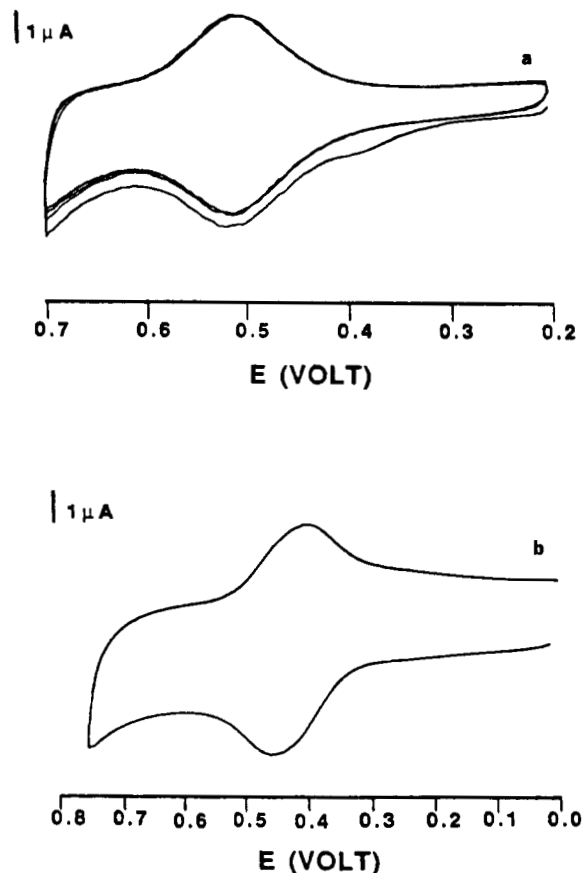$Ru(H_2O)(NH_3)_5(PF_6)_2$. If the chemisorbed staffane rods were all tilted regularly at ~45° away from normal, one of the thiol groups would be available for functionalization.

(viii) Electrochemistry of Films of Types D and E. In Figure 9 the electrochemical properties of a neat film of [2]6, adsorbed from 1 mM solution in MeCN (type D), are compared with those of a 2 mM solution of [2]6 at a glassy carbon electrode in 1 M $HClO_4$. Results obtained with a film of type E obtained by metalation of film C were identical and are not shown. A glassy carbon electrode was used in the solution experiments because the complex adsorbs on noble metal electrodes. The peak currents for both the oxidation and reduction of the immobilized [2]6 varied linearly with scan rate over scan rates of 25 mV s^{-1} to 50 V s^{-1}. The peak potential (E_p) of the immobilized material of 0.51 V vs SCE, at $\nu = 200$ mV s^{-1}, is about 60 mV more positive than that of the solution species. This suggests that the Ru(II) in the film is stabilized with respect to Ru(III), which may be attributed to an increased electrostatic interaction between the Ru-centers in the +3 oxidation state. Alternatively, the shift in peak potential of the film may be a consequence of the differences in specific ion pairs formed between the electroactive group and the ClO_4^- ions from the supporting electrolyte.[19] The charge passed under the anodic wave, after background correction, was ~12 μC cm^{-2} (geometric area of electrode) or 1.2×10^{-10} mol cm^{-2}. The densest commensurate packing of the Ru–staffane molecules would be $2(\sqrt{3} \times \sqrt{3})R30°$, which affords 83 Å^2 per molecule projected area per $Ru(NH_3)_5^{2+}$ center or 2.0×10^{-10} mol cm^{-2} per monolayer. The roughness of the polycrystalline Au substrate used was 1.6 ± 0.2, as determined by the charge passed for the reduction of an adsorbed iodine monolayer on bare Au.[32] Thus, the observed

(32) (a) Bravo, B. G.; Michelhaugh, S. L.; Soriaga, M. P.; Villegas, I.; Suggs, D. W.; Stickney, J. L. *J. Phys. Chem.* **1991**, *95*, 5245. (b) Rodriguez, J. F.; Soriaga, M. P. *J. Electrochem. Soc.* **1988**, *135*, 616. (c) Rodriguez, S. P.; Mebrahtu, T.; Soriaga, M. P. *J. Electroanal. Chem.* **1987**, *233*, 283.
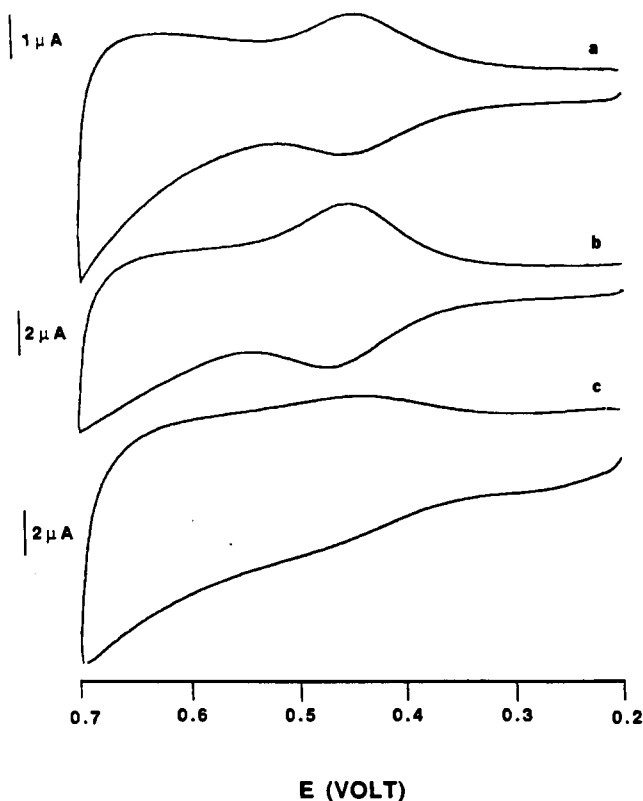
[n]Staffane-3,3$^{(n-1)}$-Dithiols

J. Am. Chem. Soc., Vol. 114, No. 25, 1992 9951

Figure 10. Cyclic voltammogram of [2]6 (film type E) on a polycrystalline gold (area = 0.18 cm^2) in (a) 0.5 M H$_2$SO$_4$, (b) 2 M CF$_3$COOH, and (c) 0.1 M HCl. ν = 200 mV s^{-1}.

coverage is equivalent to about 0.4 monolayer of Ru(NH$_3$)$_5$$^{2+}$, which is similar to that observed by Finklea and Hanshew for HS(CH$_2$)$_n$(C=O)—NH—CH$_2$—pyRu(NH$_3$)$_5$(PF$_6$)$_2$ (n = 10, 11, 15) SAM on polycrystalline Au prepared by similar techniques.[14c] The relatively low coverage can probably be attributed to electrostatic repulsions among the Ru(NH$_3$)$_5$$^{2+}$ centers, as well as the need to accommodate counterions. This would be similar for films D and E. If we assume that the divalent counterions (or half of the monovalent ions) are a part of the 2($\sqrt{3}$ × $\sqrt{3}$)R30° array, the observed coverage is, within experimental error, a complete monolayer of Ru(NH$_3$)$_5$$^{2+}$ and anions.

The choice of supporting electrolyte had a significant effect on the electrochemical behavior. The cyclic voltammograms of the same electrode, covered with a film of [2]6 (type E) formed in situ from a film of type C, in 0.5 M H$_2$SO$_4$, in 2 M HTFA, and in 0.1 M HCl are compared in Figure 10. The electrochemical properties of the film appear to depend on the nature of the anion in the supporting electrolyte; both the redox potential and the reversibility of the electron exchange, as indexed by i_a/i_c, changed with the electrolyte anion. No redox waves were observed in 0.1 M HPF$_6$ or 0.1 M NH$_4$PF$_6$ solutions, but waves were observed when the [2]6–Au electrode was transferred from these solutions into a 1 M HClO$_4$ solution.

Well-defined voltammograms were obtained for both immobilized and solution Ru–staffane species only in acidic media (pH < 2–5). For example, no waves were seen in 0.1 M NaClO$_4$, in contrast to the results in 1.0 M HClO$_4$. The variation of the oxidation peak potentials for both the surface immobilized and dissolved [2]6, measured by differential pulse voltammetry, as a function of pH of the supporting electrolyte is displayed in Figure 11. The peak potentials decreased monotonically with increasing pH in the pH range 0.0 to ~1.0. These observations suggest that a protonation—deprotonation equilibrium of the coordinated sulfur atom is associated with the redox process. Ru(II), in combination with such standard ligands as ammines, forms more stable metal–heteroatom bonds than Ru(III). The Ru(III) complex apparently loses protons rather readily; this can be attributed to the decreased electron density on the heteroatom due to dimished
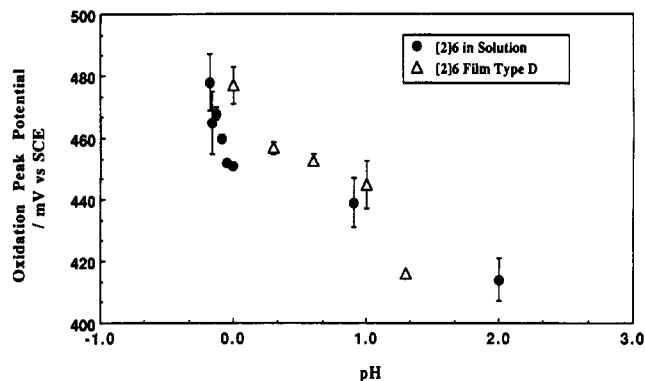

Figure 11. Variation of the oxidation peak potential (E_p) for both dissolved and surface immobilized [2]6 (film types D and E) in 1 M HClO$_4$. ν = 200 mV s^{-1}.
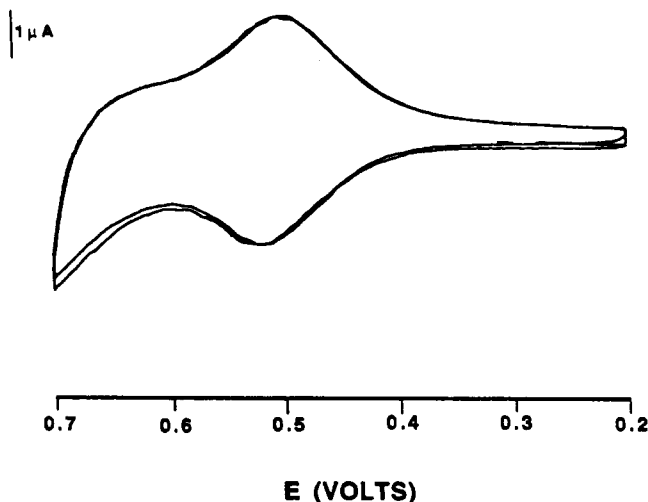

Figure 12. Cyclic voltammogram of [2]6 coadsorbed with C$_5$H$_{11}$SH (film type F) on polycrystalline gold (area = 0.18 cm^2) in 1 M HClO$_4$. ν = 200 mV s^{-1}.
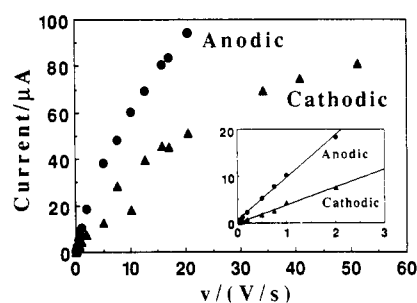

Figure 13. Cyclic voltammetric peak current as a function of scan rate for [2]6 coadsorbed with n-C$_5$H$_{11}$SH (film type F) on polycrystalline gold (area = 0.18 cm^2) in 1 M HClO$_4$.

backbonding with increased metal oxidation state.[33,34] Thus, it appears that the observed film properties depend on both the extent of anion penetration and the position of the thiol–thiolate equilibrium of the Ru-coordinated sulfur atom. Above pH ~1.0 the correlation between the peak potentials and pH became erratic and no waves were observed at pH > 3.0.

(ix) Electrochemistry of Mixed [n]6 and RSH Films (Type F). Figure 12 shows the cyclic voltammogram of a film produced by coadsorbing [2]6 and n-C$_5$H$_{11}$SH onto a polycrystalline Au electrode in 1.0 M HClO$_4$. The redox potential of the ruthenium complex in the mixed film is identical to that in the neat film ($E°$ ~ 0.51 V vs SCE), and the full peak width at half height ($\Delta E_{p1/2}$)

(33) Watt, G. D. *J. Am. Chem. Soc.* **1972**, *94*, 7351.
(34) Kuehn, C. G.; Taube, H. *J. Am. Chem. Soc.* **1976**, *98*, 689.

9952

J. Am. Chem. Soc. **1992**, *114*, 9952–9959

of ~90 mV suggests that the immobilized electroactive centers do not interact.[9a] The decrease in charging current at the foot of the wave (compare with Figure 9) on addition of n-$C_5H_{11}SH$ suggests a more tightly packed film and less anion penetration in the presence of the alkane thiol. The peak current varied linearly with scan rate up to ~2.0 V s^{-1}, (Figure 13 insert) and then deviated from linearity at faster scan rates (Figure 13); compare to films of neat [2]6, where linearity was found up to 50 V s^{-1}. Similar results were obtained for mixed films of [2]6 and n-$C_{10}H_{21}SH$. These results can be understood in terms of heterogeneous electron transfer rate limitations between the electrode and Ru-group becoming important at high scan rates in the mixed films. Thus if the alkyl thiols chemisorb preferentially on the gold substrate to form a first monolayer film onto which the Ru–staffane complex then adsorbs, the Ru-group would be spaced further from the electrode surface. Under these conditions, electron exchange between the immobilized complex and the substrate in the layered structure will be hampered by the insulating alkyl thiol layer.

The coadsorbed [n]6 exchanged with pure RSH when an electrode first coated with [n]6 was exposed to a solution of the latter. After being exposed to 0.1 mM $C_5H_{11}SH$ in MeCN for 48 h, the cyclic voltammogram of the same electrode showed a peak current ~10^6 times smaller than that in the unexchanged voltammogram.

Conclusions

Self-assembled films of the rigid-rod dithiols [n]4 on gold are disordered, presumably because some of the rods lie and some stand on the surface. They have poor electrode blocking properties. In contrast, self-assembled films of the rigid-rod thiol–thiol acetates [n]5 and ruthenium complexes [n]6 are highly ordered, with the rods perpendicular to the surface, and have excellent blocking properties. Hydrolysis removes the surface acetyl groups from the outer surface of the film assembled from [n]5 without detectable damage to the film or change in the orientation of the rods, and subsequent functionalization with ruthenium pentaammine is possible. The resulting electroactive film has electrochemical properties identical to those of the film self-assembled from [n]6 but has a lower density of the supporting rods. The electrochemical properties of the ruthenated films depend on the pH and on the nature of the supporting electrolyte.

Intramolecular Magnetic Coupling between Two Nitrene or Two Nitroxide Units through 1,1-Diphenylethylene Chromophores. Isomeric Dinitrenes and Dinitroxides Related in Connectivity to Trimethylenemethane, Tetramethyleneethane, and Pentamethylenepropane

Takuya Matsumoto, Takayuki Ishida, Noboru Koga, and Hiizu Iwamura*

Contribution from the Department of Chemistry, Faculty of Science, The University of Tokyo, 7-3-1 Hongo, Tokyo 113, Japan. Received April 27, 1992

Abstract: Isomeric vinylidenebis(phenylnitrenes) (N) and 1,1-bis[(N-oxy-*tert*-butylamino)phenyl]-2-methylpropenes (O) have been prepared, and their EPR fine structures and/or effective magnetic moments have been determined over a wide temperature range. The data were analyzed in terms of Bleaney–Bowers-type equations to give the energy gaps between the quintet and singlet states for N and the triplet and singlet states for O. They were ≫0 cm^{-1}, −42.0 cm^{-1} (−502 J/mol), a negative value representing a singlet ground state), and −26.2 cm^{-1} (−313 J/mol), and 10.6 cm^{-1} (127 J/mol), −1.8 cm^{-1} (−22 J/mol), and −3.4 cm^{-1} (−41 J/mol) for p,p'-, m,p'- and m,m'-dinitrenes N and dinitroxides O, respectively. A consistent reduction in the effective intramolecular exchange integrals J's between the two open-shell centers in the latter series is ascribed to the lower spin polarization on the phenyl rings of the dinitroxides relative to the dinitrenes. Whereas the ferro- and antiferromagnetic couplings in the p,p' and m,p'-topology are consistent not only with the Ovchinnikov's but also Borden–Davidson's rules, the antiferromagnetic interaction in the m,m'-substitution pattern is contradictory to the former and consistent with the latter theory. Since the p,p', m,p', and m,m' isomers are related to trimethylenemethane (4), tetramethyleneethane (5), and pentamethylenepropane (6), respectively, the results obtained in this work are consistent with the triplet ground state of 4. 5 and 6 are suggested to have ground singlet states. Radical centers X should be all at the para position for designing super-high-spin polyacetylenes 1 and polydiacetylenes 2.

As a part of our efforts to design and construct new organic polymers in high-spin ground states,[1] we became interested in knowing if poly(phenylacetylenes) 1 and poly(phenyldiacetylenes) 2 carrying free radical centers X as pendants on the phenyl rings would be high-spin and how strong the electron spins in X could couple each other in the polymer molecules. Experimental results

on such polymers so far reported are unsatisfactory or only partly successful[2] in contrast to well-characterized high-spin ground states

---

(1) Iwamura, H. *Adv. Phys. Org. Chem.* **1990**, *26*, 179.

(2) Fujii, A.; Ishida, T.; Koga, N.; Iwamura, H. *Macromolecules* **1991**, *24*, 1077. Inoue, K.; Koga, N.; Iwamura, H. *J. Am. Chem. Soc.* **1991**, *113*, 9803. Nishide, H.; Yoshioka, N.; Inagaki, K.; Tsuchida, E. *Macromolecules* **1988**, *21*, 3119. Nishide, H.; Yoshioka, N.; Kaneko, T.; Tsuchida, E. *Macromolecules* **1990**, *23*, 4487. Yoshioka, N.; Nishide, H.; Tsuchida, E. *Mol. Cryst. Liq. Cryst.* **1990**, *190*, 45.